Research Article GU J Sci 38(1): x-x (2025) DOI: 10.35378/gujs.1433792

Gazi University

Journal of Science

http://dergipark.gov.tr/gujs

Determination Of The Effects Of Catalyst Components On The Total Oxidation Of Methane In Zeolite Supported Catalysts Prepared By The Impregnation Method

Filiz DEREKAYA*, Bestegül HORASAN

Gazi University, Engineering Faculty, Chemical Engineering Department, 06570 Maltepe, Ankara, Türkiye

Highlights

- The effects of catalysts composition on activity were determined.
- SAPO34 support was found more suitable for the total oxidation of methane.
- ZrO_2 promoter component increased total oxidation activity of methane.

Article Info

Received: 09 Feb 24
Accepted: 27 Jun 24

Keywords

Methane
Oxidation
Zeolite
Preparation

Abstract

The aim of this study is the determination of effects of catalysts components on the methane total oxidation activities of zeolite supported catalysts. For this reason, SAPO34 and Zeolite 13X were used as zeolite support. PdO, CeO_2, ZrO_2 catalysts components were used as active component and as promoter component. Catalysts were prepared by using the impregnation method. Characteristic properties were determined by using X-Ray Diffraction, N_2 adsorption/desorption and Scanning Electron Microscopy analysis. According the characteristic results, to obtain high surface area SAPO34 should be chosen as support. According to the total methane oxidation catalytic activity studies SAPO34 supported catalysts were more active than Zeolite 13X supported catalysts. Through catalytic activity studies, the type of promoter and support component most compatible with PdO was determined. It was found that PdO-ZrO_2/SAPO34 catalyst is determined as the most active catalyst. Based on the results, it can be said that the internal interaction between PdO and ZrO_2 is better than the internal interaction between PdO - CeO_2, and that the PdO -CeO_2-ZrO_2 pair is more compatible for methane oxidation in the support structure.

1. INTRODUCTION

Methane is the main component of natural gas and contains less carbon than other carbon-intensive fossil fuels. Therefore, it emits less CO_2 during energy production than other carbon-containing compounds [1]. Methane gas is a much more effective greenhouse gas than carbon dioxide gas. For the last 20 years, the impact of methane on global warming has been stated to be 81 times greater than carbon dioxide (GWP20 = 81.1). The most effective method to eliminate this harmful effect of methane gas is the complete catalytic oxidation of methane ($CH_4 + 2O_2 \rightarrow CO_2 + 2H_2O$, $\Delta Hrxn = -891$ kJ/mol). As a result of the total catalytic oxidation of methane gas, CO_2, which is a less effective greenhouse gas, is formed. [2, 3] Palladium is known to be the most effective metal for the total oxidation of methane [3]. But it is an expensive noble metal. For this reason, it is present in very low amounts in the catalyst structure. Literature studies have shown that promoter components are used in order to increase the activity of low amounts of palladium. Therefore, in our study, depending on the catalyst composition designed in the structure of the catalyst in addition to palladium, CeO_2 components were used to ensure oxygen mobility during the oxidation reaction and ZrO_2 components were used to increase the catalyst thermal resistance. The methods chosen in catalyst synthesis are very important. The parameters during catalyst preparation (pH, temperature, mixing and surfactant, etc.) are very important for the characteristic properties of the catalyst and, accordingly, its catalytic activities.

*Corresponding author, e-mail: filizb@gazi.edu.tr

Literature studies were examined. Literature studies were examined. There are limited studies with similar content in the literature. The total oxidation of methane gas is a reaction that does not harm the environment and produces only water and much less harmful carbon dioxide. Different catalysts which contain metals, metaloxides, perovskites have been used for the catalytic oxidation of methane. Among these, palladium-containing catalysts are best for methane oxidation [4, 5]. In the catalysts used for this aim, noble metals were used with different oxide supports which have high surface area, porosity and thermal resistance [4]. In studies in which Pd-containing catalysts were used PdO was found more active than Pd for methane oxidation. Pd was formed at high temperatures cause the loss of activity [4, 5 - 8]. Cerium is the most used as promoter. CeO_2 lead to increase in dispersion of the noble metal, enhance the noble metal oxidation, increasing the reducibility of the noble metal during the reaction, increase the thermal stability of the support, release oxygen from the surface and bulk phase or supplying oxygen to the voids on the surface and bulk phase [7, 9]. In general, it has been determined that the components added to the structure besides Al_2O_3 are TiO_2, CeO_2, ZrO_2 [4, 5, 9-12]. There are a limited number of studies in the literature where zeolite support and promoter components are used together. Literature studies showed that acidic zeolite type should be preferred as support in the total oxidation of methane. Accordingly, Zeolite 13X and SAPO-34 zeolite types were selected as support for this study. According to literature research, SAPO-34 (cabazite) zeolite type has been determined to be used in the selective catalytic reduction reaction of NOx in the presence of ammonia, in the conversion reaction of biomethanol to light olefins, in the conversion reaction of methanol to ethylene, and in the cracking reaction of naphtha. The reasons for using SAPO-34 type zeolite in the studies are also stated [13, 14]. According to the literature studies, no scientific study has been found examining the effects of SAPO34 and Zeolite 13X zeolite support types and the compatibility of booster components with PdO on the catalytic activity for the total oxidation of methane. In this regard, the data in this study will contribute to the literature on the total oxidation of methane.

In this study a series of catalyst developed to oxidize and remove dilute amounts of methane using zeolite support. In literature studies conducted in this direction, two different types of zeolite (Zeolite 13X and cabazite-SAPO-34) were used as support, palladium metal was used as the active metal, and the CeO_2-ZrO_2 binary component was used to strengthen the catalyst structure against thermal conditions and increase oxygen mobility. Catalysts were prepared by surfactant-assisted impregnation method. Characterization studies and catalytic activity studies were carried out.

2. MATERIAL METHOD

2.1. Catalysts Preparation

In this study, catalysts containing PdO, PdO-CeO_2, PdO-ZrO_2 and PdO-CeO_2-ZrO_2 components in the structure supported by SAPO34 and Zeolit13X zeolite types were synthesized. The catalysts compositions are given in Table 1.

Table 1. *Catalysts and their compositions*

Catalysts	Weight Percentage
PdO/Zeolite Support	5% Pd-95% Zeolite Support
PdO-CeO_2/ Zeolite Support	5% Pd-25% CeO_2-70% Zeolite Support
PdO-ZrO_2/ Zeolite Support	5% Pd-25% ZrO_2-70% Zeolite Support
PdO-CeO_2-ZrO_2/ Zeolite Support	5% Pd-12.5% CeO_2-2.5% ZrO_2-% 70 Zeolite Support

SAPO34 zeolite support was synthesized in our study. The following chemicals were used during the preparation: tetraethylammonium hydroxide, powdered silica, aluminum isopropoxide, 1 M NaOH solution. The steps followed during the synthesis were described by Kılınç and Derekaya is given in detail

in his study [15]. Zeolite13X (Sigma) was purchased and pretreated with NH_4OH to increase its acidic properties. Kılınc et al. 's study, the NH_4OH solution treatment steps used for ZSM5 zeolite support were also followed for Zeolit13X [15].

The steps followed in the preparation of the catalyst are shown schematically in Figure 1. $Pd(NO_3)_2$ (Sigma & Aldrich, 99%), $Ce(NO_3)_2.6H_2O$ (Sigma & Aldrich, 99%), $Zr(NO_3)_2.xH_2O$ (Sigma & Aldrich, 99%), starting salts were used to obtain the active component and promoter component crystal phases in the catalyst structure. According to the catalyst structure, aqueous solution was first prepared using these metal salts and deionized water. According to the n(CTAB)/n(metal (Pd+Ce+Zr)) molar ratio, the mole amount of CTAB was calculated and added to the aqueous solution. For example, if this ratio is 1, it will be understood that the molar ratio of CTAB compared to Pd+Ce+Zr is 0.1. After the mixture was stirred at room temperature for 3 hours, the evaporation of the solvent water was carried out in a controlled manner. The solution was first dried at 40°C overnight and then at 100°C overnight. The resulting material was calcined at 500°C for 3 hours.

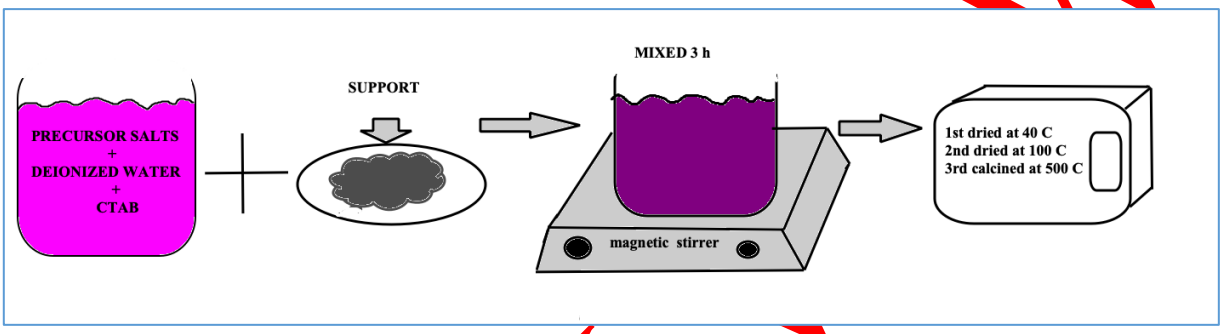

Figure 1. *The steps of the catalysts preparation with impregnation method*

2.2. Catalysts Characterization

Various characterization techniques were used for structural features of catalysts and adsorbents. All analyzes were carried out at the accredited Middle East Technical University Central Research Laboratory using the service procurement item in the project budget. Surface area, pore sizes and volumes were determined by using N_2 Adsorption/Desorption Analysis. Average crystal sizes and phases were determined by X-Ray Diffraction analysis. Surface morphology was examined with Scanning Electron Microscopy (SEM).

2.3. Methane total oxidation catalytic activity studies

Detailed information about the experimental system and reaction conditions in which methane oxidation was carried out is given in Derekaya and Bulagay [16] Reaction takes place at atmospheric pressure and reaction temperatures changes between 100°C –600°C. The quartz tubular reactor was used. Reaction feed gas composition was prepared by using 10/90 CH_4/He, 100% O_2, 100% He gas / gas mixture. Analysis of the gas mixture used as feed and the gas mixture released at the end of the reaction made by using Gas Chromograph of which detailed information given by Derekaya and Bulagay [16]. Catalytic activity system can be seen from (Figure 2). Methane conversion was calculated using the Equation (1) given below:

$$\% \, CH_4 \text{ conversion} = ((CH_4)_0-(CH_4)_f)/(CH_4)_0 \quad (1)$$

Here:
$[CH_4]_0$= Methane molar amount present in feed gas stream
$[CH_4]_f$= Methane molar amount present in effluent gas stream.

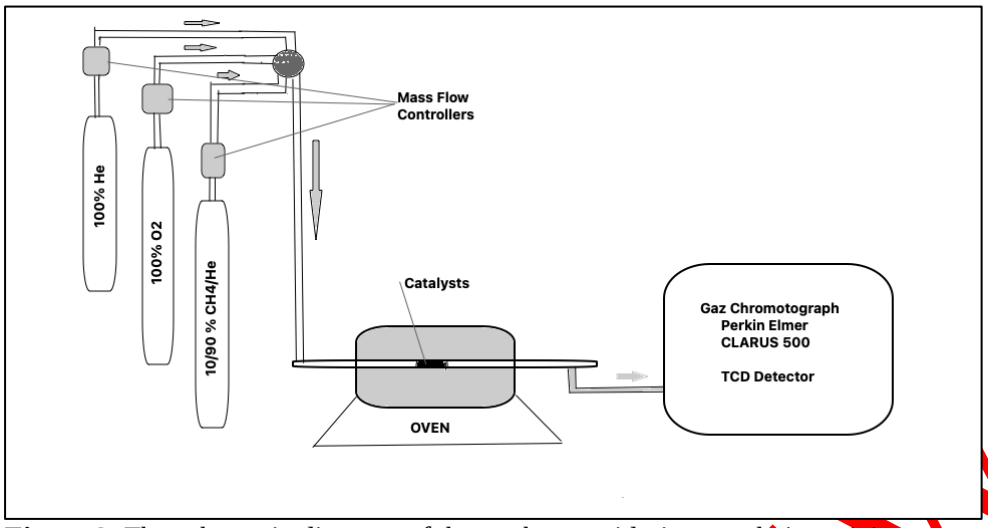

Figure 2. *The schematic diagram of the methane oxidation catalytic activity system*

3. RESULTS AND DISCUSSION

3.1. X-Ray Diffraction Analysis

XRD analysis was used to assigned the crystalline phases present in the structure. Figures 3-4 show the XRD patterns of the catalysts. Figure 3 shows the XRD patterns of the Zeolite 13X supported catalysts. The diffraction peaks determined at angles of 2θ= 7.186°, 10.160°, 12.463°, 16.099°, 20.404°, 21.679°, 24.083°, 26.131°, 27.155°, 30.061°, 30.826°, 32.543°, 33.386°, 34.172°, 35.932°, 36.485°, 38.02°, 41.81°, 44.155°, 47.542°, 52.79°, 54.276°, 69.26° originate from the Zeolite 13X support component (JCPDS card No- 44-0003). The result obtained is in agreement with the studies in the literature [17-21]. Figure 3 shows the XRD patterns of the Zeolite 13X supported catalysts. According to the XRD analysis results of the Pd/Zeolite13X catalyst, the PdO crystal phase gave diffraction peaks at angles of 2θ = 33.529°, 40.053°, 41.85°, 54.69°, 60.17°, 60.71°, 71.29°. According to the XRD analysis results of the PdO-CeO_2/Zeolite13X catalyst, the CeO_2 crystal phase gave diffraction peaks at angles of 2θ = 29.98° and 47.35°. PdO crystal phase gave diffraction peaks at angles of 2θ= 32.58°, 33.88°, 35.84°, 40.13°, 41.90°, 52.66°, 54.71°, 71.42°. In the XRD analysis of the PdO-ZrO_2/Zeolite13X catalyst, the diffraction peaks of the ZrO_2 crystal phase are at angles 2θ= 30.3°, 60.12°, 60.709° and the diffraction peaks of the PdO crystal phase are obtained at 2θ= 33.834°, 60.12°, 60.709° and 71.93° angles. According to the X-Ray diffraction pattern analysis of the PdO-CeO_2-ZrO_2/Zeolite13X catalyst, the CeO_2 crystal phase in this catalyst is at angles 2θ = 29.977°, 47.93°; ZrO_2 crystal phase at angles 2θ= 42.02°, 52.62°, 60.19°, 60.80°; PdO crystal phase was observed at angles of 2θ= 33.858°, 40.24°, 54.689°, 60.19°, 60.80°, 71.41°. Pd crystal phase gave a diffraction peak at an angle of 2θ = 46.53°.

Figure 4 shows the XRD patterns of the Zeolite SAPO34 supported catalysts. The diffraction peaks determined at angles 2θ = 9.53°, 18.123°, 20.31°, 20.52°, 21.42°, 21.403°, 22.89°, 35.30°, 37.544°, 39.785°, 40.63°, 44.891°, 47.822°, 51.28°, 53.15°, 64.632° originate from the SAPO34 Zeolite support. As a result of the literature studies, it was observed that it was fully compatible with the characteristic SAPO-34 peaks [22]. From XRD analysis of PdO/SAPO34 catalyst, the PdO crystal phase gave diffraction peaks at angles of 2θ = 33.50°, 33.85°, 40.09°, 41.914°, 54.67°, 60.16°, 60.78° and 71.38°. Pd crystal phase gave diffraction peaks at 2θ= 46.65° and 68.09°. In the X-Ray diffraction pattern analysis of PdO-CeO_2/SAPO34 catalyst, CeO_2 crystal phase gives a diffraction peak at 2θ= 28.72° angle, while PdO crystal phase gives 2θ= 33.50°, 33.84°, 54.70°, 60.20°, 71.18°, 71.49°. gave diffraction peaks at different angles. In the X-Ray diffraction pattern analysis of PdO-ZrO_2/SAPO34 catalyst, ZrO_2 crystal phase gives diffraction peaks at angles of 2θ= 41.87°, 46.71°, 60.20°, 60.85°, while PdO crystal phase gives diffraction peaks at angles of 2θ= 33.53°, 33.84°, 46.71°, 60.20°, 60.85°, 71.27°. According to the XRD analysis result of Pd-CeO_2-ZrO_2/SAPO34 catalyst, CeO_2 crystal phase is at angles 2θ= 29.13°, 46.08°, 48.10°; ZrO_2 crystal phase gave diffraction

peaks at angles of 2θ= 31.20°, 41.93°, 60.16°, 60.82° and PdO crystal phase gave diffraction peaks at angles of 2θ= 33.84°, 54.68°, 60.16°, 60.82° and 71.33°. The results obtained show that the desired crystal phase structure has been achieved in the catalysts. Diffraction peak angles of PdO, Pd, CeO_2 and ZrO_2 crystal phases are in agreement with studies in the literature.

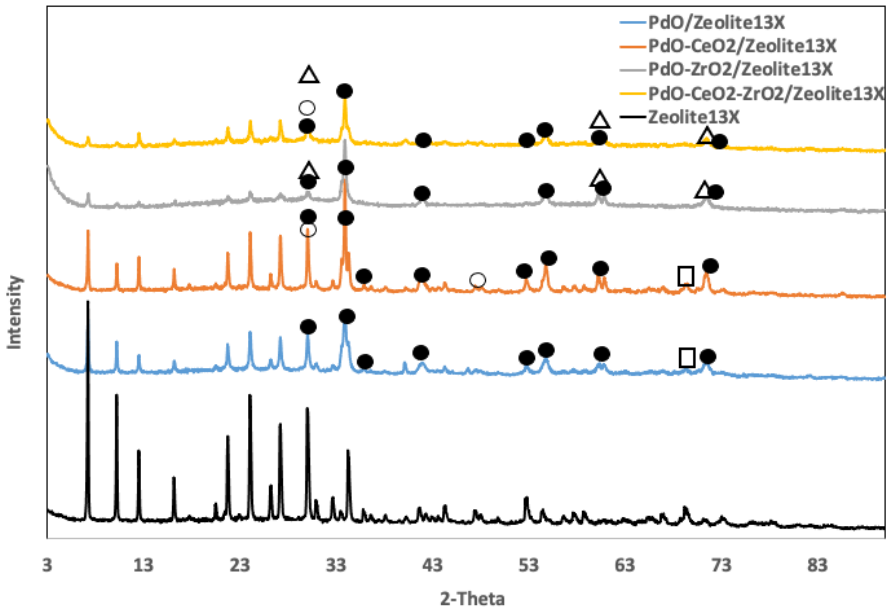

Figure 2. *The XRD patterns of the Zeolite13X supported catalysts (Pd:□ , PdO:● , CeO_2: ○, ZrO_2:△)*

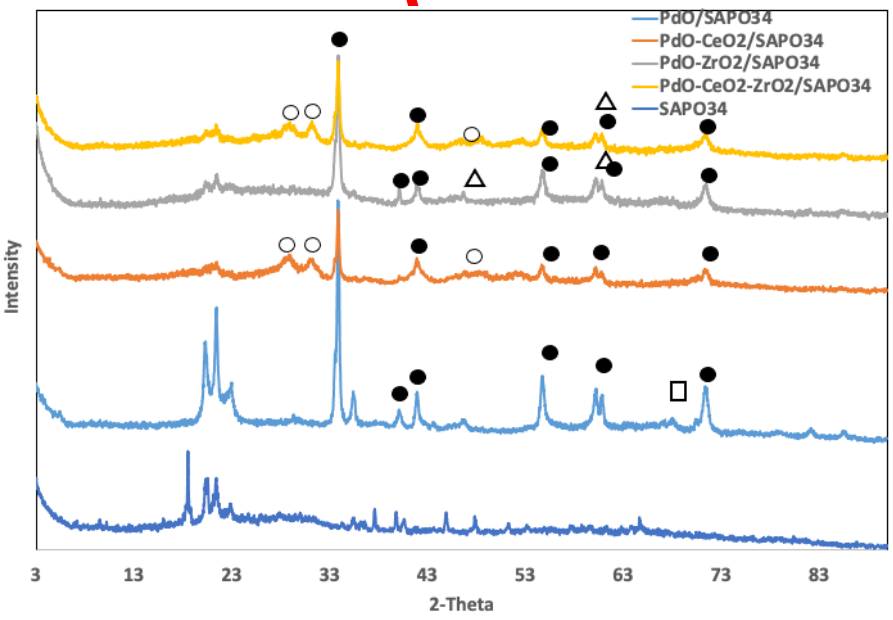

Figure 3. *The XRD patterns of the SAPO34 supported catalysts (Pd:□ , PdO:● , CeO_2: ○, ZrO_2:△)*

3.2. N_2 Adsorption/Desorption Analysis

Since the multipoint test is more reliable it was used in this study to determine the surface areas of the catalysts. Table 2 shows the multipoint surface area values of the catalysts. Higher surface areas were obtained from SAPO34 zeolite-supported catalysts, and the surface areas increased with the introduction of metal oxide into the structure. The best elevation was obtained in catalysts with PdO-ZrO_2 composition supported by both ZrO_2-containing zeolite types. It is understood from the results given in Table 2 that the

CeO_2-ZrO_2 catalyst component are more positive for the surface area result than the catalysts that only have PdO and PdO-CeO_2 in the structure. In this case, it turns out that PdO-ZrO_2 catalyst component pair and SAPO34 zeolite support type are the best catalyst components for surface area.

Table 2. *Surface areas and pore diameters of all catalysts*

Catalysts / Zeolite Support	Surface Area, m^2/g	
	SAPO34	Zeolite13X
PdO/Zeolite	40.10	14.85
PdO-CeO_2/Zeolite	105.6	11.64
PdO-ZrO_2/Zeolite	191.6	81.00
PdO-CeO_2-ZrO_2/Zeolite	142.6	67.67

Figure 5 shows the N_2 adsorption/desorption isotherms of the cayalysts. According to the IUPAC classification, N_2 adsorption desorption isotherms of the catalysts comply with TYPE V. Type IV and V isotherms are obtained from materials with mesoporous structure according to this classification. H3 hysteresis type was observed in SAPO34 supported catalysts and H4 hysteresis type was observed in Zeolite13X supported catalysts. Materials that give rise to H3 hysteresis have slit-shaped pores. Type H4 hysteresis is also often associated with narrow slit pores [23].

Table 3 shows the Total Pore Volume and Meso+Micro Pore Volumes of the catalysts. The Meso+Micro pore volumes are greater than the macro pore volume. The increase in meso+micro pore volume was obtained when the ZrO_2 was introduced to catalysts structure. Results showed that the percentage of the meso+micro pore volume is greater of which catalysts composition is PdO-ZrO_2/Zeolite in both Zeolite13X and SAPO34 zeolite supported catalysts. Like surface area results, for high meso+micro pore volume results the SAPO34 zeolite support and PdO-ZrO_2 catalyst component should choosen.

Table 3. *Pore Volumes of all catalysts*

Catalysts	$V_{Micro+Meso}$	V_{Total}	$V_{Micro+Meso}$	V_{Total}
	V≡ cm^3/g,liquid N_2 , STP			
	SAPO34		Zeolite13X	
PdO/Zeolite	0.10	0.15	0.026	0.03
PdO-CeO_2/Zeolite	0.29	0.43	0.029	0.05
PdO-ZrO_2/Zeolite	0.41	0.46	0.075	0.08
PdO-CeO_2-ZrO_2/Zeolite	0.49	0.65	0.101	0.12

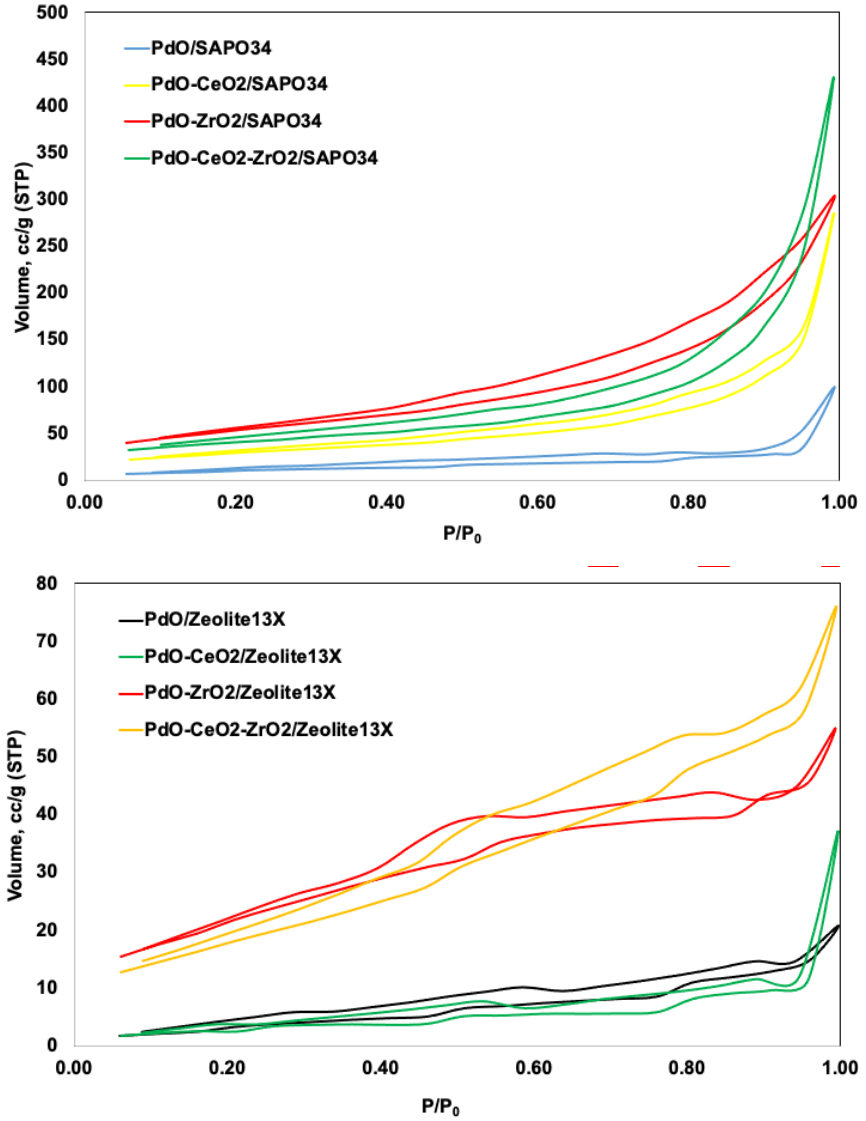

Figure 5. *N_2 adsorption/desorption isotherms of the catalysts*

Table 4 and Figures 6-7 shows the average pore diameters and pore size distribution of the catalysts. Catalysts have a mesoporous structure. Big pores which are close to macropore boundary were also obtained from SAPO34 zeolite supported catalysts. The closest results to uniform porosity were obtained from Zeolite13X supported PdO-ZrO_2 and PdO-CeO_2-ZrO_2 catalysts. Average pore diameter results with more than one value were due to the zeolites used as supports. Surface areas vary depending on the type of support. In this study, SAPO34 zeolite support allowed obtaining higher surface area from catalysts. Although the surface area of the PdO-CeO_2-ZrO_2/SAPO34 catalyst is lower than the PdO-ZrO_2/SAPO34 catalyst, both the total pore volume and meso+micro pore volume are higher. This result can be attributed to the larger area under the curve in the microporosity region of the PdO-ZrO_2/SAPO34 catalyst, as seen in Figure 7. Micropores caused the surface area to increase. This had a positive effect on the activity of the catalyst. The structure of SAPO34 is similar to the chabazite zeolite type and has the advantages of providing high surface area and high porosity [24, 25]. It is also reported in the literature that the high surface area decreases with the addition of metal to the SAPO34 structure. Because the small pores are filled with metal components [26]. In a study in the literature, it was stated that the surface area of 4 wt% Pd/CeO_2 catalyst was 32.4 m^2/g [27]. In this case, in this study, it was determined that preparing both Zeolite

13X and SAPO34 zeolite support types including PdO and CeO_2 had a positive effect on the surface area result.

Table 4. *Average pore diameters of all catalysts*

Catalysts / Zeolite Support	Average Pore Diameter, nm	
	SAPO34	Zeolite13X
PdO/Zeolite	2.1, 2.7, 3.3, 4.2-6.3, 9.1, 40	2.4, 3.7, 6.3-16.0
PdO-CeO_2/Zeolite	2.4, 3.9, 4.9, 9.4, 17.6	1.9, 2.4, 3.7, 6.4, 16.1
PdO-ZrO_2/Zeolite	3.8, 5.6, 9.7, 17.6	2.1, 3.4, 5.5
PdO-CeO_2-ZrO_2/Zeolite	4.3, 6.5, 17.9, 31.9	3.0, 3.8, 5.6, 17.4

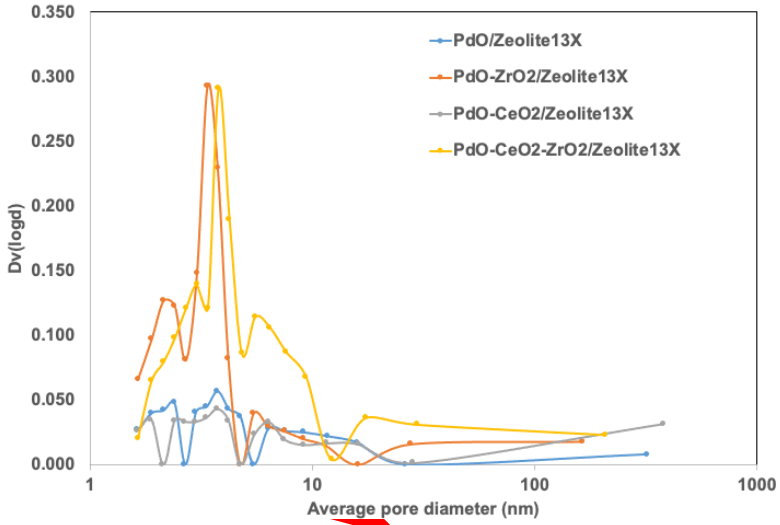

Figure 6. *The pore diameter distribution of the Zeolite13X supported catalysts*

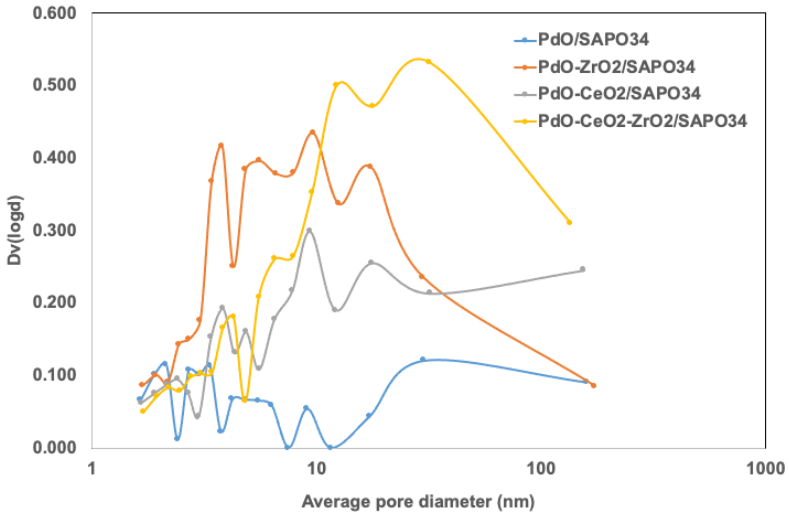

Figure 7. *The pore diameter distribution of the SAPO34 supported catalysts*

3.3. Scanning Electron Microscopy (SEM)

Figures 8-9 show the SEM images of the PdO/Zeolite13X and PdO-ZrO_2/Zeolite13X catalysts. As stated in the study of Guedes et al., it has been determined that the surface structure of the catalysts has irregular shapes and sizes, mostly rock structure [28]. Surface images of both catalysts show that PdO and PdO-ZrO_2 catalyst components are very well distributed in the Zeolite13X support structure. Very small spherical particles were formed on the support surface. It can be seen that there are no voids on the surface, and the active component and support component are distributed homogeneously on the support surface.

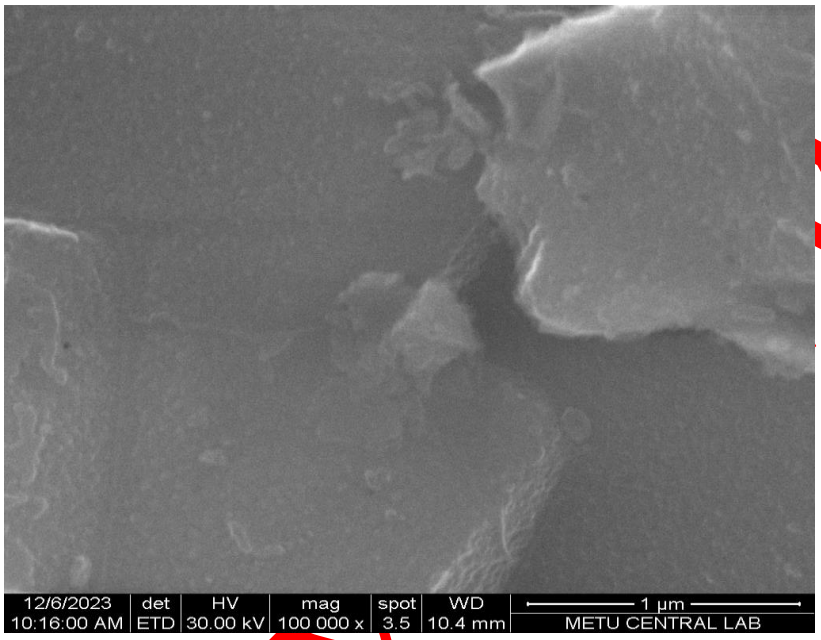

Figure 8. *The SEM image of PdO/Zeolite13X catalyst*

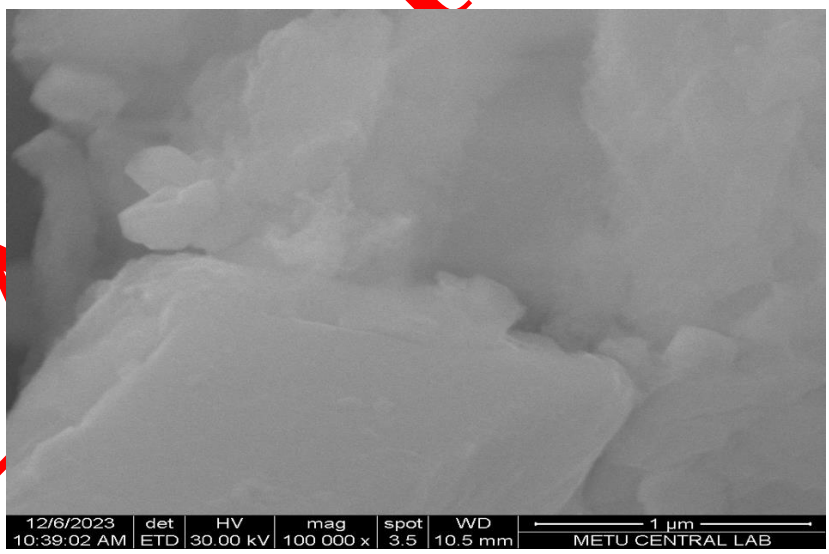

Figure 9. *The SEM image of PdO-ZrO_2/Zeolite13X catalyst*

3.4. Catalytic Activity

Table 5 shows the methane conversion data depending on the reaction temperature obtained from the methane oxidation activity experiments of SAPO 34 supported catalysts. The lowest activity among SAPO 34 catalysts was obtained from the PdO/SAPO34 catalyst (Figure 10). It gave the highest conversion at 600°C and this result was below 10%. Adding CeO_2 next to PdO affected the activity positively. PdO-CeO_2/SAPO34 catalyst gave 39% methane conversion at the highest temperature of 600°C. It showed very low methane conversion between 1% and 5% between temperatures of 100-500°C. Adding ZrO_2 next to PdO created a more positive result in activity than adding CeO_2. PdO-ZrO_2/SAPO34 catalyst gave methane conversion between 1% and 25% between 200-500°C temperatures. Methane conversion increased after 500°C and exhibited 70% methane conversion at 600°C. Based on the results, it can be said that the internal interaction between PdO and ZrO_2 is better than the internal interaction between PdO and CeO_2, and that the PdO and ZrO_2 pair is more compatible for methane oxidation in the support structure. In the presence of the PdO component and CeO_2 and ZrO_2, methane conversion was not observed between temperatures of 100-500°C. But transformation was achieved at 500°C and above. The methane conversions obtained from the PdO-ZrO_2/SAPO34 catalyst and the results obtained from the PdO-CeO_2-ZrO_2/SAPO34 catalyst are very close. In this case, the additional presence of CeO_2 in the PdO-ZrO_2/SAPO34 structure did not affect the methane conversion results much. Considering the catalyst cost, it is concluded that PdO-ZrO_2/SAPO34 catalyst is the most active catalyst among the SAPO34 supported and prepared catalysts by impregnation method.

Table 6 shows the methane conversion data depending on the reaction temperature obtained from the methane oxidation activity experiments of Zeolite13X supported catalysts. Catalytic activity graphs showing methane conversion as a function of temperature are shown in Figure 11. Generally low methane conversion was obtained from Zeolite13X supported catalysts. Among the Zeolite13X supported catalysts, the highest PdO-CeO_2/Zeolite13X catalyst was obtained. While this catalyst did not show activity up to 400°C, it showed methane conversion activity starting from this temperature. Approximately 75% methane conversion was achieved from this catalyst at 600°C. The second best activity among Zeolite13X supported catalysts was obtained from the PdO/Zeolite13X catalyst. This catalyst showed no activity up to 500°C, but its activity increased after this temperature and gave 65% methane conversion at the highest temperature of 600°C. 50% methane conversion was achieved from PdO/Zeolite13X and PdO-CeO_2/Zeolite13X catalysts at approximately 519°C. In this case, according to the conversion results obtained at 600°C reaction temperature, the presence of the CeO_2 component next to PdO had an increasing effect on the activity of Zeolite13X supported catalysts.

There are no studies in the literature that directly include the catalyst components used in this study and on the total oxidation of methane. The catalytic activity results were evaluated by comparing the results of studies with similar content on the catalyst structures in our study. Miller et.al. studied the total oxidation of methane over a series of Pd catalysts supported on: Al_2O_3, ZrO_2–CeO_2 and CeO_2. They observed the catalytic activity order over the catalysts as Pd/Al> Pd/ZrCe> Pd/Ce. They concluded that activity is related to the relative density of PdO–Pd* active site pairs on the catalyst surface [29]. Roth et.al studied the effect of particle size of Pd on total oxidation of methane over Pd/Al_2O_3 catalysts. They found that for particles of size lower than 12 nm, the catalytic activity was constant while for larger particles, it decreased with increasing particle size [8]. Osman et al. synthesized palladium and platinum bimetallic catalyst with η-Al_2O_3, ZSM-5(23) and ZSM-5(80) supports using the wet impregnation method in the presence and absence of TiO_2 in the structure. The results obtained showed that for a highly active and stable catalyst, all four components (palladium, platinum, acidic support and oxygen carrier) must be present in the structure. It has been stated that the optimum support is 17.5% TiO_2/ZSM-5(80) and the 10% transformation temperature over this support is 200°C [30].

Table 5. *Methane conversion data of SAPO 34 supported catalysts*

T °C	PdO/SAPO34	PdO-CeO_2/SAPO34	PdO-ZrO_2/SAPO34	PdO-CeO_2-ZrO_2/SAPO34
100	-	0.1	-	-
200	-	-	0.7	-
300	-	0.8	2.6	-
400	-	1.7	5.5	-
500	0.5	5.6	24.8	28.9
600	8.9	39	70.1	72.5

Table 6. *Methane conversion data of Zeolite13X supported catalysts*

T°C	PdO/ *Zeolite13X*	PdO-CeO_2/ *Zeolite13X*	PdO-ZrO_2/ *Zeolite13X*	PdO-CeO_2-ZrO_2/ *Zeolite13X*
100	-	-	0.64	-
200	-	-	-	-
300	-	-	-	-
400	8.6	11.7	-	-
500	44.6	48.2	1.8	2.7
600	64.9	74.9	23.1	18.5

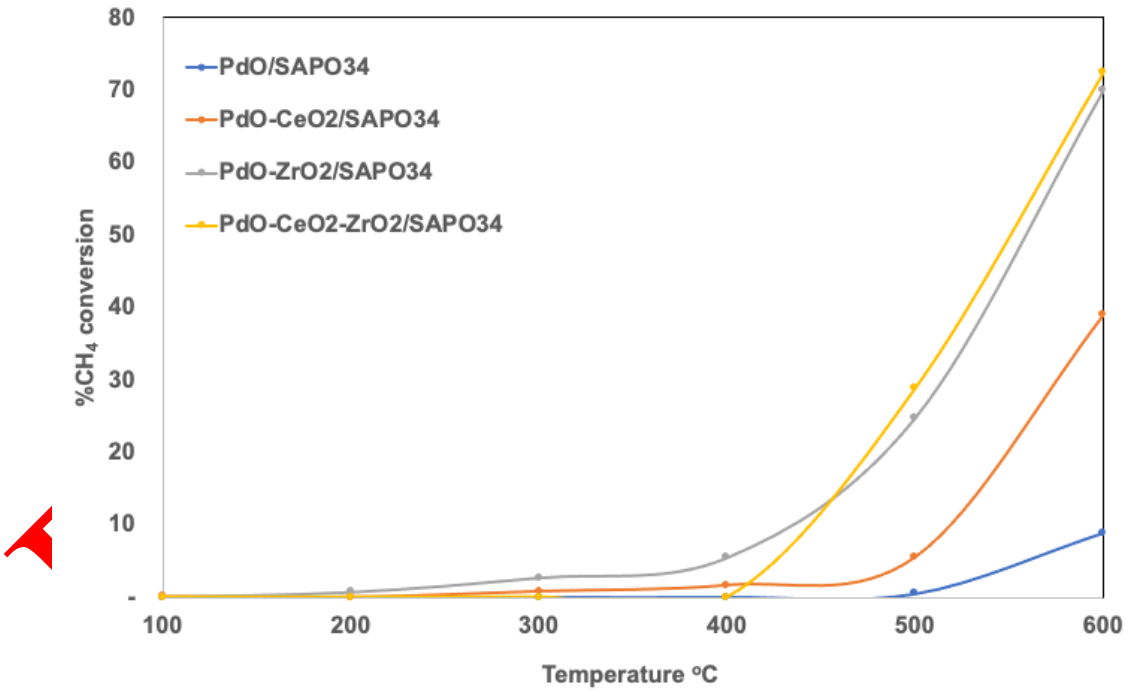

Figure 10. *The catalytic activity results over the SAPO34 supported catalysts (%1CH_4, %21 O_2 and balance with He; 25 mg catalysts; 25ml/min flow rate)*

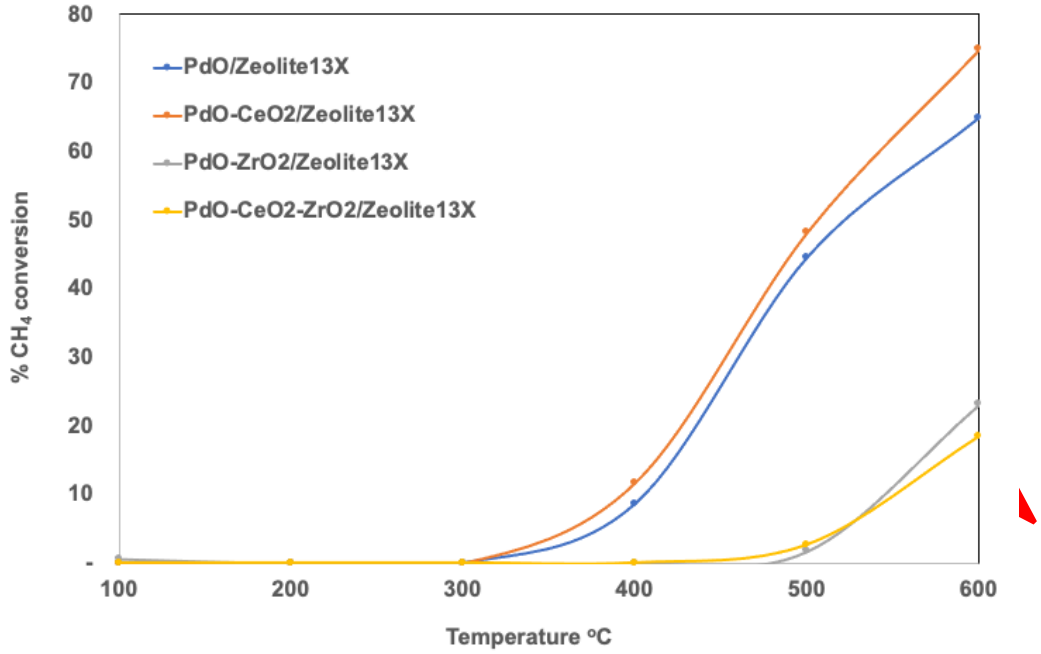

Figure 11. *The catalytic activity results over the Zeolite13X supported catalysts (%1CH_4, %21 O_2 and balance with He; 25 mg catalysts; 25ml/min flow rate)*

4. CONCLUSION

In this study, the total oxidation of methane was examined using catalysts supported by different zeolite types and containing different components. SAPO34 and Zeolite 13X were used as zeolite support. SAPO34 was synthesized within the scope of the study, but Zeolite 13 X was purchased and pretreated only with ammonia solution. While PdO was kept constant as the active component in the catalyst structure, the effects of CeO_2, ZrO_2 and CeO_2+ZrO_2 promoter components added to the structure on both structural and activity properties were examined. Catalysts were synthesized by the impregnation method. X-Ray diffraction analaysis of the catalysts which was used to determine the crystal phases presents in catalyst structure showed that PdO, CeO_2 and ZrO_2 crystal phases were obtained according to the catalyst composition. Some catalysts also showed diffraction peaks originating from the Pd metallic crystal phase. Surface areas, average pore diameters, pore volume results were obtained from N_2 Adsorption/Desorption analysis. Higher surface areas were obtained from SAPO34 zeolite-supported catalysts, and the surface areas increased with the introduction of metal oxide into the structure. Meso+micro pore volumes were obtained higher than macro pore volumes. Big pores which are close to macropore boundary were also obtained from SAPO34 zeolite supported catalysts. According to the SEM analysis there are no voids on the surface, and the active component and support component are distributed homogeneously on the support surface for PdO-ZrO_2/Zeolite13X catalyst. All catalysts were tested for total oxidation of methane. Among the SAPO34 supported catalysts lowest activity was obtained from the PdO/SAPO34 catalyst. The PdO-ZrO_2/SAPO34 catalyst showed highest activity among the SAPO34 supported catalysts. Generally low methane conversion was obtained from Zeolite13X supported catalysts. Among the Zeolite13X supported catalysts, the highest activity was obtained on PdO-CeO_2/Zeolite13X catalyst.

In future studies, the effects of different parameters on the same catalysts, both on the structural properties of the catalysts and on their activity properties for the total oxidation of methane, can be examined. The same catalysts can be synthesized by a method other than the impregnation method. Catalysts can be calcined at a different temperature. The proportions of the components in the gas mixture used in the total oxidation of methane can be changed.

ACKNOWLEDGEMENTS

This work has been supported by Gazi University Scientific Research Projects Coordination Unit under grant number BAP 06/2020-06. Studies related to the hydrothermal synthesis method belong to my master's student Bestegül HORASAN's thesis.

CONFLICTS OF INTEREST

No conflict of interest was declared by the authors.

REFERENCES

[1] Majumdar, S.S., Moses-DeBusk, M., Deka, D.J., Kidder, M.K., Thomas, C.R., Pihl, J.A., " Impact of Mg on Pd-based methane oxidation catalysts for lean-burn natural gas emissions control", Applied Catalysis B: Environmental, 341: 123253, (2024)

[2] Mortensen, R.L., Noack, H.D., Pedersen, K., Dunstan, M.A., Wilhelm, F., Rogalev, A., Pedersen, K.S., Mielby, J., Mossin, S., "Understanding the reversible and irreversible deactivation of methane oxidation catalysts", Applied Catalysis B: Environment and Energy, 344: 123646 (2024).

[3] Friberg, I., Sadokhina, N., Olsson, L., "The effect of Si/Al ratio of zeolite supported Pd for complete CH4 oxidation T in the presence of water vapor and SO_2", Applied Catalysis B: Environmental, 250: 117-131 (2019).

[4] Lovón-Quintan J.J., Santos, J.B.O, Lovón, A.S.P, La-Salvia, N., Valenc ¸G.P., "Low- temperature oxidation of methane on Pd-Sn/Zr_{O2} catalysts", Journal of Molecular Catalysis A: Chemical, 411: 117–127, (2016).

[5] Lin, W., Zhu, Y.X., Wu, N.Z.,Xie, Y.C., Murwani, I., Kemnitz, E., "Total oxidation of methane at low temperature over Pd/TiO_2/Al_2O_3: effects of the support and residual chlorine ions", Applied Catalysis B: Environmental, 50: 59–66, (2004).

[6] Marceau, E., Lauron-Pernot, H., Che, M., "Influence of the Metallic Precursor and of the Catalytic Reaction on the Activity and Evolution of Pt(Cl)/δ-Al_2O_3 Catalysts in the Total Oxidation of Methane", Journal of Catalysis, 197: 394 –405, (2001).

[7] Lin, W., Lin, L., Zhu, Y.X., Xie, Y.C., Scheurell, K., Kemnitz, E., "Novel Pd/TiO_2–ZrO_2 catalysts for methane total oxidation at low temperature and their 18O-isotope exchange behavior", Journal of Molecular Catalysis A: Chemical, 226: 263–268, (2005).

[8] Roth, D., Ge´lin, P., Kaddouri, A., Garbowski, E., Primet, M.,Tena, E., "Oxidation behaviour and catalytic properties of Pd/Al_2O_3 catalysts in the total oxidation of methane", Catalysis Today, 112: 134–138, (2006).

[9] Rami´rez-Lo´pez, R., Elizalde-Martinez, I., Balderas-Tapia, L., "Complete catalytic oxidation of methane over Pd/CeO_2–Al_2O_3:The influence of different ceria loading", Catalysis Today, 150: 358–362, (2010).

[10] Miller, J.B., Malatpure, M., "Pd catalysts for total oxidation of methane: Support effects", Applied Catalysis A: General, 495: 54–62, (2015).

[11] Sadokhina, N., Smedler, G., Nylén, U., Olofsson, M., Olssona, L., "The influence of gas composition on Pd-based catalyst activity in methane oxidation − inhibition and promotion by NO", Applied Catalysis B: Environmental, 200: 351–360, (2017).

[12] Bozo, C., Guilhaume, N., Herrmanny, J.M., "Role of the Ceria–Zirconia Support in the Reactivity of Platinum and Palladium Catalysts for Methane Total Oxidation under Lean Conditions", Journal of Catalysis, 203: 393–406, (2001).

[13] Wang, F., Ren, J., Cai, Y., Sun, L., Chen, C., Liang, S., Jiang, X., "Palladium nanoparticles confined within ZSM-5 zeolite with enhanced stability for hydrogenation of p- nitrophenol to p-aminophenol", Chemical Engineering Journal, 283: 922–928, (2016).

[14] Aghaei, E., Haghighi, M., "Enhancement of catalytic lifetime of nanostructured SAPO- 34 in conversion of biomethanol to light olefins", Microporous and Mesoporous Materials, 196: 179–190, (2014).

[15] Kılınç, Y.S., Derekaya, F., "CO Methanation Over SAPO-34 Supported Ni Catalysts", Gazi University Journal of Science Journal of Science, 36(4): 1480-1494, (2023).

[16] Derekaya, B. F., Bulagay, E., "Total Oxidation of Methane over the $LaNi_{1-x}MxO_3$ (M: Mn, Ag, Cu, Co) Perovskites", Arabian Journal for Science and Engineering, 47(5): 6325-6339, (2022).

[17] Qiu, C., Wang, S., Gao, R., Qin, J., Li, W., Wang, X., Zhai, Z., Tian, D., Song, Y., "Low-temperature synthesis of PdO-CeO_2/C toward efficient oxygen reduction reaction", Materials Today Energy, 18: 100557, (2020).

[18] Zhang, L., Ding, L.X., Luo, Y., Zeng, Y., Wang, S., Wang, H., "PdO/Pd-CeO_2 hollow spheres with fresh Pd surface for enhancing formic acid oxidation", Chemical Engineering Journal, 347: 193-201, (2018).

[19] Huang, F., Chen, J., Hu, W., Li, G., Wu, Y., Yuan, S., Zhong, L., Chen, Y., "Pd or PdO: Catalytic active site of methane oxidation operated close to stoichiometric air-to-fuel for natural gas vehicles", Applied Catalysis B: Environmental, 219: 73-81, (2017).

[20] Zahra, T., Ahmad, K. S., Zequine, C., Gupta, R. K., Thomas, A. G., Malik, M. A., Jaffri, S. B., Ali, D., "Electro-catalyst [ZrO_2/ZnO/PdO]-NPs green functionalization: Fabrication, characterization and water splitting potential assessment", Int. Journal of Hydrogen Energy, 46: (37), 19347-19362, (2021).

[21] Colussi, S., Trovarelli, A., Vesselli, E., Baraldi, A., Comelli, G., Groppi, G., Llorca, J., "Structure and morphology of Pd/Al_2O_3 and Pd/CeO_2/Al_2O_3 combustion catalysts in Pd–PdO transformation hysteresis", Applied Catalysis A: General, 390: 1-10, (2010).

[22] Li, G., Wang, B., Sun, Q., Xu, W. Q., Ma, Z., Wang, H., Zhang, D., Zhou, J., "Novel Synthesis Of Fly-Ash-Derived Cu-Loaded SAPO-34 Catalysts And Their Use İn Selective Catalytic Reduction Of NO With NH_3", Green Energy & Environment, 4: 470-482, (2019).

[23] ALOthman, Z.A., "A Review: Fundamental Aspects of Silicate Mesoporous Materials", Materials, 5: 2874-2902, (2012).

[24] Passamonti, F.J., Benitez, V.M., Especel, C., Epron, F., Pieck, C. L., D´Ippolito, S. A., "SiO_2-Al_2O_3 catalysts for methanol to olefins: Comparative study with SAPO34 and ZSM5", Applied Catalysis A: General, 670: 119556, (2024).

[25] Simonetti, M., Gentile, V., Fracastoro, G.V., Freni, A., Calabrese, L., Chiesa, G., "Experimental testing of the buoyant functioning of a coil coated with SAPO34 zeolite, designed for solar DEC (Desiccant Evaporative Cooling) systems of buildings with natural ventilation", Applied Thermal Engineering, 103: 781-789, (2016).

[26] Mousavi, Y.S., Akbari, A., Omidkhah, M., Safari, P., "Formulated Mn-promoted SAPO-34/kaolin/alumina sol micro-size catalyst with a superior performance for methanol to light olefins conversion in a fluidized bed reactor", Journal of Industrial and Engineering Chemistry, 129: 403-412, (2024).

[27] Kwon, G., Kim, G., Lee, H., "Continuous methane to ethane conversion using gaseous oxygen on ceria-based Pd catalysts at low temperatures", Applied Catalysis A: General, 623: 118245, (2021).

[28] Guedes, J.M., Fernandes, F.R.D., Batista dos Santos, A.P., Martins dos Santos Neto, M., Teixeira, A.M.R., Marinho, E.S., Alencar de Menezes, J.E.S., Garcia, K.G.V., Santos, A.G.D., Silva dos Santos, H., "NiO and ZrO_2 impregnation in KIT-6 by excess solvent and mechanochemistry: A comparison", Materials Letters, 345: 134512, (2023).

[29] Miller, J.B., Malatpure, M., "Pd catalysts for total oxidation of methane: Support effects", Applied Catalysis A: General, 495: 54-62, (2015).

[30] Osman, A.I. Abu-Dahrieh, J.K., Laffir, F., Curtin, T., Thompson, J.M., Rooney, D.W., "A bimetallic catalyst on a dual component support for low temperature total methane oxidation", Applied Catalysis B: Environmental, 187: 408-418, (2016).